Transactions of NAS of Azerbaijan, Issue Mechanics, **38** (7), 43–55 (2018).
Series of Physical-Technical and Mathematical Sciences.

3D non-axisymmetric dynamic interface shear stress field in the elastic system consisting of the hollow cylinder and surrounding elastic medium

Mahir A. Mehdiyev

Received: 30.08.2018 / Revised: 10.10.2018 / Accepted: 15.11.2018

Abstract. *This paper is a continuation of the paper "Akbarov SD and Mehdiyev MA. (2018) "The interface stress field in the elastic system consisting of the hollow cylinder and surrounding elastic medium under 3D non-axisymmetric forced vibration", CMC: Computers, Materials & Continua 54 (1): 61 - 81" in which it was proposed and employed the solution method for investigation of the 3D non-axisymmetric dynamic problems for the bi-material elastic system consisting hollow cylinder and surrounding infinite elastic medium. However, in the aforementioned paper, the concrete investigations are made for the interface normal stress only. Therefore, in the present paper, the aforementioned investigations and discussions are made for the interface shear stresses. Numerical results on the frequency responses of the mentioned shear stresses are presented and discussed .*

Keywords. Forced vibration · frequency response · interface shear stresses · Fourier transform · Fourier series

Mathematics Subject Classification (2010): 74B05, 42A38, 74H45

1 Introduction

First of all, we note that the detailed review of the related investigations are given in the papers [3, 4, 8, 12] and in the monograph [5] therefore we do not consider here this review again. Nevertheless, we review here some recent results which have been obtained with the participation of the author of the present paper and begin this review with the paper [1] in which the axisymmetric interface stress state in the "hollow cylinder surrounding elastic medium" under action in the interior the time-harmonic ring forces. The dynamics of the moving ring load acting in the interior of the cylinder surrounded by an elastic medium in the axisymmetric case has been studied in the paper [8]. In the paper [8] the problem considered in the [8] is studied in the case where in the "hollow cylinder - surrounding elastic system" there exist the homogeneous initial stresses caused by the initial static forces

M.A. Mehdiyev
Institute of Mathematics and Mechanics of NAS of Azerbaijan, Baku
Azerbaijan State University of Economics, (UNEC), Baku, Azerbaijan
E-mail: mahirmehdiyev@mail.ru

acting at infinity in the cylinder's axis direction. 3D non-axisymmetric dynamics of the moving load acting on the interior of the hollow cylinder surrounded by the elastic medium has been investigated in the paper [3]. The 3D non-axisymmetric forced vibration of the aforementioned bi-material system is considered in the paper [4] and it is studied the interface normal stress only. However, the working carrying capacity as well as the adhesion strengths of the system consisting of the hollow cylinder and surrounding elastic medium depend also significantly on the interface shear stresses. Therefore in the present paper, the investigations, started in the paper [4] is developed, and the aforementioned interface shear stresses are studied. Numerical results on the frequency response of these stresses and the influence of the problem parameters on these responses are presented and discussed.

2 Formulation of the problem and solution method

Note that the formulation of the problem is the same as in the paper [4], nevertheless for readability of the paper briefly we repute this formulation Note that the formulation of the problem is the same as in the paper [4], nevertheless, for readability of the paper we repute briefly this formulation and consider the system the sketch of which is illustrated in Fig. 1.

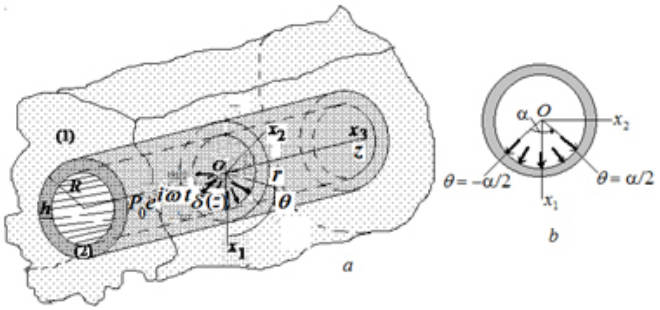

Fig. 1. The sketch of the system under consideration and non-axisymmetric time-harmonic forces acting in the interior of the hollow cylinder (a) and the cross-section of the cylinder (b) and the distribution of the amplitude of the external forces in the circumferential direction

Note that the formulation of the problem is the same as in the paper [4], nevertheless for readability of the paper briefly we repute this formulation Note that the formulation of the problem is the same as in the paper [4], nevertheless, for readability of the paper we repute briefly this formulation and consider the system the sketch of which is illustrated in Fig. 2.1.

As shown in Fig. 2.1 the thickness of the cylinder is h and the external radius of the cross-section of this cylinder is R. We associate the cylindrical system of coordinate with the axis of the cylinder and assume that in the interior of the cylinder the point located with respect to the cylinder axis and non-uniformly distributed in the circumferential direction time-harmonic normal forces act. Moreover, assume that the materials of the cylinder and surrounding elastic medium are homogeneous and isotropic. Within these frameworks we investigate the non-axisymmetric frequency response of the system to the time-harmonic external forces.

As in [4], below, we denote the values related to the hollow cylinder and to the surrounding elastic medium with the upper indices (2.2) and (2.1) respectively.

Thus, we write the field equations, relations and boundary and contact conditions in the selected cylindrical system of coordinates.

Equations of motion:

$$\frac{\partial\sigma_{rr}^{(m)}}{\partial r}+\frac{1}{r}\frac{\partial\sigma_{r\theta}^{(m)}}{\partial\theta}+\frac{\partial\sigma_{rz}^{(m)}}{\partial z}+\frac{1}{r}(\sigma_{rr}^{(m)}-\sigma_{\theta\theta}^{(m)})=\rho^{(m)}\frac{\partial^2u_r^{(m)}}{\partial t^2},$$

$$\frac{\partial\sigma_{r\theta}^{(m)}}{\partial r}+\frac{1}{r}\frac{\partial\sigma_{\theta\theta}^{(m)}}{\partial\theta}+\frac{\partial\sigma_{z\theta}^{(m)}}{\partial z}+\frac{2}{r}\sigma_{r\theta}^{(m)}=\rho^{(m)}\frac{\partial^2u_\theta^{(m)}}{\partial t^2},$$

$$\frac{\partial\sigma_{rz}^{(m)}}{\partial r}+\frac{1}{r}\frac{\partial\sigma_{z\theta}^{(m)}}{\partial\theta}+\frac{\partial\sigma_{zz}^{(m)}}{\partial z}+\frac{1}{r}\sigma_{rz}^{(m)}=\rho^{(m)}\frac{\partial^2u_z^{(m)}}{\partial t^2}. \tag{2.1}$$

Elasticity relations:

$$\sigma_{rr}^{(m)}=(\lambda^{(m)}+2\mu^{(m)})\frac{\partial u_r^{(m)}}{\partial r}+\lambda^{(m)}\frac{1}{r}(\frac{\partial u_\theta^{(m)}}{\partial r}+u_r^{(m)})+\lambda^{(m)}\frac{\partial u_z^{(m)}}{\partial z},$$

$$\sigma_{\theta\theta}^{(m)}=\lambda^{(m)}\frac{\partial u_r^{(m)}}{\partial r}+(\lambda^{(m)}+2\mu^{(m)})\frac{1}{r}(\frac{\partial u_\theta^{(m)}}{\partial r}+u_r^{(m)})+\lambda^{(m)}\frac{\partial u_z^{(m)}}{\partial z},$$

$$\sigma_{zz}^{(m)}=\lambda^{(m)}\frac{\partial u_r^{(m)}}{\partial r}+\lambda^{(m)}\frac{1}{r}(\frac{\partial u_\theta^{(m)}}{\partial r}+u_r^{(m)})+(\lambda^{(m)}+2\mu^{(m)})\frac{\partial u_z^{(m)}}{\partial z},$$

$$\sigma_{r\theta}^{(m)}=\mu^{(m)}\frac{\partial u_\theta^{(m)}}{\partial r}+\mu^{(m)}(\frac{1}{r}\frac{\partial u_r^{(m)}}{\partial\theta}-\frac{1}{r}u_\theta^{(m)}),$$

$$\sigma_{z\theta}^{(m)}=\mu^{(m)}\frac{\partial u_\theta^{(m)}}{\partial z}+\mu^{(k)}\frac{\partial u_z^{(m)}}{r\partial\theta},\sigma_{zr}^{(k)}=\mu^{(k)}\frac{\partial u_r^{(k)}}{\partial z}+\mu^{(k)}\frac{\partial u_z^{(k)}}{\partial r}. \tag{2.2}$$

In (2.1) and (2.2) the conventional notation is used.

It follows from the foregoing assumptions and from the Fig. 1b that it can be written the following boundary conditions on the interior surface of the hollow cylinder.

$$\sigma_{rr}^{(2)}\Big|_{r=R-h}=\begin{cases}-P_\alpha e^{i\omega t}\delta(z) & \text{for } -\alpha/2\le\theta\le\alpha/2\\ 0 & \text{for } \theta\in([-\pi,+\pi]-[-\alpha/2,\alpha/2])\end{cases},$$

$$\sigma_{r\theta}^{(2)}\Big|_{r=R-h}=0,\ \sigma_{rz}^{(2)}\Big|_{r=R-h}=0. \tag{2.3}$$

where P_α is determined from the following relation.

$$\int_{-\alpha/2}^{+\alpha/2}P_\alpha(R-h)\cos\theta d\theta=(R-h)P_0\ =const\ \Rightarrow\ P_\alpha=P_0/2\sin(\alpha/2). \tag{2.4}$$

It is assumed that the perfect contact conditions satisfy and these conditions are written as follows.

$$\sigma_{rr}^{(2)}\Big|_{r=R}=\sigma_{rr}^{(1)}\Big|_{r=R},\ \sigma_{r\theta}^{(2)}\Big|_{r=R}=\sigma_{r\theta}^{(1)}\Big|_{r=R},\ \sigma_{rz}^{(2)}\Big|_{r=R}=\sigma_{rz}^{(1)}\Big|_{r=R},$$

$$u_r^{(2)}\Big|_{r=R}=u_r^{(1)}\Big|_{r=R},\ u_\theta^{(2)}\Big|_{r=R}=u_\theta^{(1)}\Big|_{r=R},\ u_z^{(2)}\Big|_{r=R}=u_z^{(1)}\Big|_{r=R}. \tag{2.5}$$

Moreover, it is assumed that assume that

$$\left\{\left|\sigma_{rr}^{(k)}\right|;\left|\sigma_{r\theta}^{(k)}\right|;...;\left|\sigma_{z\theta}^{(k)}\right|;\left|u_{r}^{(k)}\right|;...;\left|u_{z}^{(k)}\right|\right\}<M, k=1,2 \text{ as } \sqrt{r^2+z^2}\to+\infty. \quad (2.6)$$

With this we exhaust the problem formulation and consider the solution method of this problem. This method is based on the use of the following representation described in [7].

$$u_r^{(m)}=\frac{1}{r}\frac{\partial}{\partial\theta}\Psi^{(m)}-\frac{\partial^2}{\partial r\partial z}\mathrm{X}^{(m)}, u_\theta^{(m)}=-\frac{\partial}{\partial r}\Psi^{(m)}-\frac{1}{r}\frac{\partial^2}{\partial\theta\,\partial z}\mathrm{X}^{(m)},$$

$$u_z^{(m)}=(\lambda^{(m)}+\mu^{(m)})^{-1}\left((\lambda^{(m)}+2\mu^{(m)})\Delta_1+\mu^{(m)}\frac{\partial^2}{\partial z^2}-\rho^{(m)}\frac{\partial^2}{\partial t^2}\right)\mathrm{X}^{(m)},$$

$$\Delta_1=\frac{\partial^2}{\partial r^2}+\frac{1}{r}\frac{\partial}{\partial r}+\frac{1}{r^2}\frac{\partial^2}{\partial\theta^2}, m=1,2, \quad (2.7)$$

where the functions $\Psi^{(m)}$ and $\mathrm{X}^{(m)}$are the solutions to the equations given below.

$$\left(\Delta_1+\frac{\partial^2}{\partial z^2}-\frac{\rho^{(k)}}{\mu^{(k)}}\frac{\partial^2}{\partial t^2}\right)\Psi^{(m)}=0, \left[\left(\Delta_1+\frac{\partial^2}{\partial z^2}\right)\left(\Delta_1+\frac{\partial^2}{\partial z^2}\right)+\right.$$

$$-\rho^{(m)}\frac{\lambda^{(m)}+3\mu^{(m)}}{\mu^{(m)}(\lambda^{(m)}+2\mu^{(m)})}(\Delta_1+\frac{\partial^2}{\partial z^2})\Big)\frac{\partial^2}{\partial t^2}+$$

$$\left.+\frac{(\rho^{(m)})^2}{\mu^{(m)}(\lambda^{(m)}+2\mu^{(m)})}\frac{\partial^4}{\partial t^4}\right]\mathrm{X}^{(m)}=0. \quad (2.8)$$

Using the presentation $f(r,\theta,z,t)=\bar{f}(r,\theta,z)e^{i\omega t}$ where $\bar{f}(r,\theta,z)$ is an amplitude of the sought value (we will omit the over-bar on the amplitudes) we can replace the operators $\partial^2/\partial t^2$ and $\partial^4/\partial t^4$ with the $-\omega^2$ and ω^4 respectively and obtain the equations, relations, boundary and contact conditions for the amplitudes of the sought values from the forgoing equations. Further, applying the exponential Fourier transform $f_F=\int\limits_{-\infty}^{+\infty}f(z)e^{i\,s\,z}dz$ with respect to the coordinate z (where s is a transform parameter) to all the equations, relations, boundary and contact conditions obtained for the amplitudes.

Thus, according to the foregoing discussions the amplitudes of the sought values can be presented through their Fourier transform by the following expressions.

$$\left\{\sigma_{rr}^{(m)};\ \sigma_{\theta\theta}^{(m)};\sigma_{zz}^{(m)};\sigma_{r\theta}^{(m)};u_r^{(m)};u_\theta^{(m)};\Psi^{(m)}\right\}=$$

$$\frac{1}{\pi}\int\limits_0^{+\infty}\left\{\sigma_{rrF}^{(m)};\ \sigma_{\theta\theta F}^{(m)};\sigma_{zzF}^{(m)};\sigma_{r\theta F}^{(m)};u_{rF}^{(m)};u_{\theta F}^{(m)};\Psi_F^{(m)}\right\}\cos(sz)ds,$$

$$\left\{\sigma_{\theta z}^{(m)};\ \sigma_{rz}^{(m)};u_z^{(m)};\mathrm{X}^{(m)}\right\}=\frac{1}{\pi}\int\limits_0^{+\infty}\left\{\sigma_{\theta zF}^{(m)};\ \sigma_{rzF}^{(m)};u_{zF}^{(m)};\mathrm{X}_F^{(m)}\right\}\sin(sz)ds. \quad (2.9)$$

We use the dimensionless coordinates $r'=r/h$ and $z'=z/h$ (the upper prime will be omitted below) and introduce the notation

$$\Omega=\frac{\omega h}{c_2^{(2)}} \quad (2.10)$$

where $c_2^{(1.2)} = \sqrt{\mu^{(1.2)}/\rho^{(1.2)}}$and call it the dimensionless frequency.

Thus, substituting the expressions in (2.9) into the foregoing equations and relations, and taking the notation (2.10) into consideration we obtain the following equations for the functions $\Psi_F^{(m)}$ and $\mathrm{X}_F^{(m)}$:

$$\left(\Delta_1 - \left(s^2 - \frac{\Omega^2 (c_2^{(2)})^2}{(c_2^{(m)})^2}\right)\right) \Psi_F^{(m)} = 0, \left[\left(\Delta_1 - s^2\right)\left(\Delta_1 - s^2\right) + \right.$$

$$\left. + \frac{\lambda^{(m)} + 3\mu^{(m)}}{\lambda^{(m)} + 2\mu^{(m)}} (\Delta_1 - s^2)\right) \frac{\Omega^2 (c_2^{(2)})^2}{(c_2^{(m)})^2} + \frac{1}{(\lambda^{(m)}/\mu^{(m)} + 2)} \frac{\Omega^4 (c_2^{(2)})^4}{(c_2^{(m)})^4}\Bigg] \mathrm{X}_F^{(m)} = 0. \quad (2.11)$$

where $c_2^{(m)} = \sqrt{\mu^{(m)}/\rho^{(m)}}$.

Taking the periodicity of the amplitudes with respect to the θ into account the functions $\Psi_F^{(m)}$ and $X_F^{(m)}$can be presented in the Fourier series form as follows.

$$\Psi_F^{(m)}(r, s, \theta) = \sum_{n=1}^{\infty} \Psi_{Fn}^{(m)}(r, s) \sin n\theta,$$

$$\mathrm{X}_F^{(m)}(r, s, \theta) = \frac{1}{2} \mathrm{X}_{F0}^{(m)}(r, s) + \sum_{n=1}^{\infty} \mathrm{X}_{Fn}^{(m)}(r, s) \cos n\theta. \quad (2.12)$$

Thus, we obtain the equations given below for the unknown functions $\Psi_{Fn}^{(m)}(r, s)$ and $X_{Fn}^{(m)}(r, s)$ from the equations (2.11) and (2.12).

$$\left(\Delta_{1n} - (\zeta_1^{(m)})^2\right) \psi_{Fn}^{(m)} = 0, \left(\Delta_{1n} - (\zeta_2^{(m)})^2\right) \left(\Delta_{1n} - (\zeta_3^{(m)})^2\right) \mathrm{X}_{Fn}^{(m)} = 0,$$

$$\Delta_{1n} = \frac{d^2}{dr^2} + \frac{d}{rdr} - \frac{n^2}{r^2}, \quad (2.13)$$

where

$$(\zeta_1^{(m)})^2 = \left(s^2 - \frac{\Omega^2 (c_2^{(2)})^2}{(c_2^{(m)})^2}\right). \quad (2.14)$$

The constants $(\zeta_2^{(m)})^2$ and $(\zeta_2^{(m)})^2$ in the equation (2.13) are determined as solutions of the following equation.

$$(\zeta^{(m)})^4 - (\zeta^{(m)})^2 \left[-\frac{\Omega^2 (c_2^{(2)})^2}{(c_2^{(m)})^2} - s^2(\lambda^{(m)}/\mu^{(m)} + 2) + \right.$$

$$\frac{\mu^{(m)}}{\lambda^{(m)} + 2\mu^{(m)}} \left(-\frac{\Omega^2 (c_2^{(2)})^2}{(c_2^{(m)})^2} - s^2\right) + s^2 \left.\frac{(\lambda^{(m)} + \mu^{(m)})^2}{\mu^{(m)}(\lambda^{(m)} + 2\mu^{(m)})}\right] + \quad (2.15)$$

$$+ s^2 \left(\frac{-1}{\lambda^{(m)}/\mu^{(m)} + 2} \frac{\Omega^2 (c_2^{(2)})^2}{(c_2^{(m)})^2} - 1\right) \left(-\frac{\Omega^2 (c_2^{(2)})^2}{(c_2^{(m)})^2} - s^2\right) = 0.$$

Taking the condition in (2.6) into consideration, the solution to the equations in (2.13) is found as follows.

For the hollow cylinder:

$$\psi_{Fn}^{(2)} = A_{1n}^{(2)} I_n(\zeta_1^{(2)} r) + B_{1n}^{(2)} K_n(\zeta_1^{(2)} r),$$

$$\chi_{Fn}^{(2)} = A_{2n}^{(2)} I_n(\zeta_2^{(2)} r) + A_{3n}^{(2)} I_n(\zeta_3^{(2)} r) + B_{2n}^{(2)} K_n(\zeta_2^{(2)} r) + B_{3n}^{(2)} K_n(\zeta_3^{(2)} r). \tag{2.16}$$

For the surrounding elastic medium:

$$[\psi_{Fn}^{(1)} = B_{1n}^{(1)} K_n(\zeta_1^{(1)} r), \chi_{Fn}^{(1)} = B_{2n}^{(1)} K_n(\zeta_2 r) + B_{3n}^{(1)} K_n(\zeta_3^{(1)} r), \tag{2.17}$$

where $I_n(x)$ and $K_n(x)$ are the modified Bessel functions of the $n-th$ order of the first and second kinds, respectively. In (2.16) and (2.17) the arguments of these functions, i.e. the $(\zeta_l^{(q)} r)$,$(l = 1, 2, 3;\ q = 1, 2)$, in the case under consideration, in general, are complex numbers. Moreover, the $B_{1n}^{(2.1}$, $B_{2n}^{(2.1)}$, $B_{3n}^{(2.1)}$ $A_{1n}^{(2.2)}$, $A_{2n}^{(2.2)}$, $A_{3n}^{(2.2)}$, $B_{1n}^{(2.2)}$ and $B_{2n}^{(2.2)}$ in (2.16) and (2.17) are unknown constants which are determined from the boundary (2.3) and contact (2.5) conditions. In this determination procedure the first condition in (2.3) is transformed to the following one

$$\sigma_{rrF}^{(2)}\Big|_{r=R-h} = \begin{cases} -P_\alpha \ \text{ for } \ -\alpha/2 \le \theta \le \alpha/2 \\ 0 \quad \text{for} \quad \theta \in ([-\pi, +\pi] - [-\alpha/2, \alpha/2]) \end{cases}, \tag{2.18}$$

which it can be presented as in a series form

$$\sigma_{rrF}^{(2)}\Big|_{r=R-h} = -\frac{\alpha}{2\pi} P_\alpha - \frac{2\sin(\alpha/2)}{\pi} P_\alpha \sum_{n=1}^{\infty} \frac{1}{n} \cos(n\theta). \tag{2.19}$$

Thus, in this way it is determined analytical expressions of the Fourier transforms of the sought values. The original of those are determined numerically with the use of the algorithm and PC programs described in the paper [4]. Therefore, we here do not consider this algorithm and PC programs and their testing and immediately go to the analysis of the related numerical results. At the same time, we note that under numerical investigations the infinite series $\sum\limits_{n=1}^{\infty}(\cdot)_n$ in (2.12) and (2.19) are replaced with the corresponding finite series $\sum\limits_{n=1}^{N}(\cdot)_n$ and the number N is determined as $N = 20$ from the convergence requirement of the numerical results.

3 Numerical results and their analysis

We consider numerical results related to the interface shear stresses

$$\sigma_{rz}(R, \theta, z) = \sigma_{rz}^{(2)}(R, \theta, z) = \sigma_{rz}^{(1)}(R, \theta, z), \tag{3.1}$$

$$\sigma_{r\theta}(R, \theta, z) = \sigma_{r\theta}^{(2)}(R, \theta, z) = \sigma_{r\theta}^{(1)}(R, \theta, z). \tag{3.2}$$

First we consider the frequency response of these stresses in the case where the shear stress $\sigma_{rz}(R, \theta, z)$is calculated at $z/h = 0.5$ and $\theta = 0$, however, the shear stress $\sigma_{r\theta}$is calculated at $z/h = 0$ and $\theta = \pi/12$. Such selection of the coordinates follows from the fact that the considered stresses their absolute maximum values obtain namely in the around of the corresponding selected points. In obtaining all numerical results which will be considered below it is assumed that $\nu^{(2.1)} = \nu^{(2.1)} = 0.3$, where through ν the Poisson's ratio of the corresponding material is denoted. Moreover, below through the letters $E$and $\rho$the modulus of elasticity and the density of the corresponding material will be denoted.

Thus, we consider the graphs given in Fig. 2 which illustrate the frequency response of the shear stress σ_{rz}in the cases where $\alpha = \pi/12$ (a), $\pi/6$(b) and $\pi/4$(c) for various values of the ratios $E^{(2.1)}/E^{(2.2)}$ $(= \rho^{(1)}/\rho^{(2.2)})$ under $R/h = 10$.

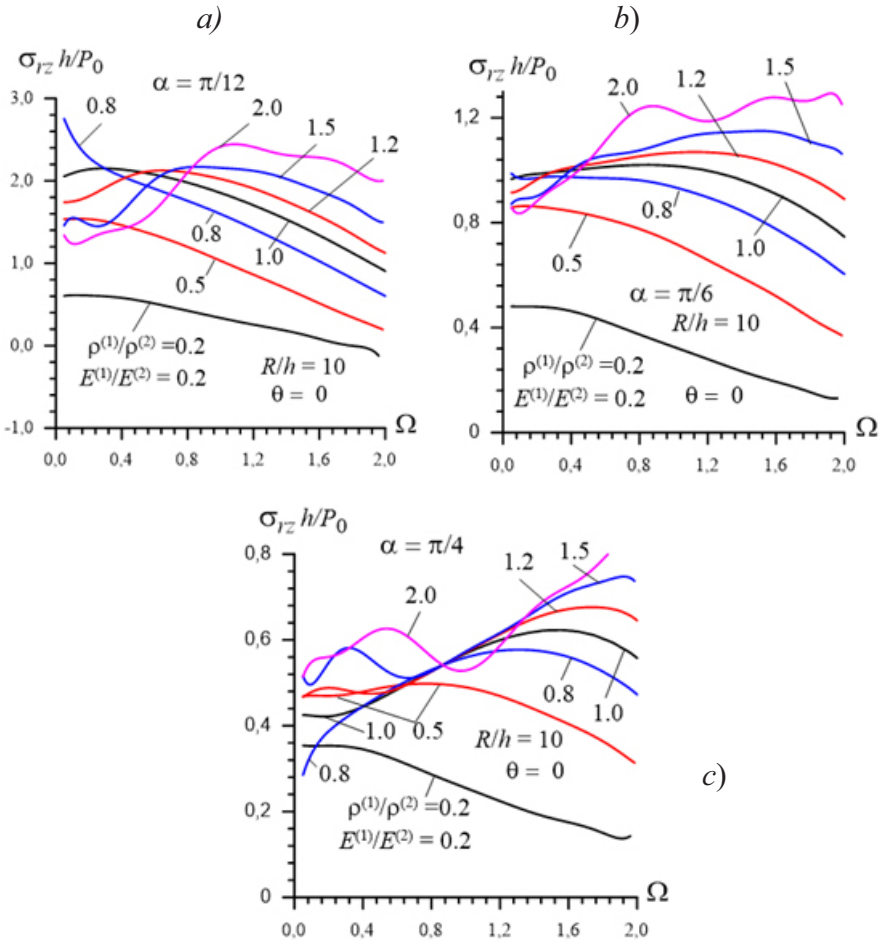

Fig. 2. Frequency response of the interface shear stress σ_{rz}in the cases where $\alpha = \pi/12(a)$, $\pi/6$ (b) and $\pi/4$(c) for various values of the ratio $E^{(1)}/E^{(2.2)}(=\rho^{(1)}/\rho^{(2.2)})$ under $R/h = 10$

It follows from these results that maximum values of the shear stress $\sigma_{rz}$with respect to Ω increase monotonically with the ratio $E^{(1)}/E^{(2)}$. This means that the maximum values of the stressσ_{rz} increase with increasing of the modulus of elasticity of the surrounding elastic medium under fixed modulus of the hollow cylinder material. The comparison of the results given in Fig. 2a, Fig. 2b and Fig. 2c with each other shows that an increase in the values of the angle α causes a decrease in the values of the shear stress σ_{rz}. Moreover, the comparison of the results given in Fig. 3 with the corresponding ones obtained in the paper [1] shows that the present results are greater significantly than those obtained in the corresponding axisymmetric case. Consequently, such results enhance the significance of the numerical results obtained in the present paper for the interface shear stresses under non-axisymmetric dynamic time-harmonic loading.

We consider also the influence of the ratio R/h on the frequency response of the shear stress σ_{rz} the results for which are given in Fig. 3 which are constructed in the cases where $E^{(1)}/E^{(2)} = \rho^{(1)}/\rho^{(2)}) = 0.5$ (Fig. 3a, Fig. 3b and Fig. 3c) and $E^{(1)}/E^{(2)} = 1.2$ (Fig. 3d and Fig. 3e) under $\alpha = \pi/12$ (Fig. 3a and Fig. 3d), $\pi/6$ (Fig. 3b and Fig. 3e) and $\pi/4$ (Fig. 3c). It follows from these results that, in general, an increase in the values of the ratio R/h causes to increase the values of the shear stress σ_{rz}. Moreover, these results show that the non-monotone character of the frequency response of the stress σ_{rz} is established with

increasing of the ratio R/h. Besides all of these the results show that the values of the σ_{rz} approach to each other with R/h.

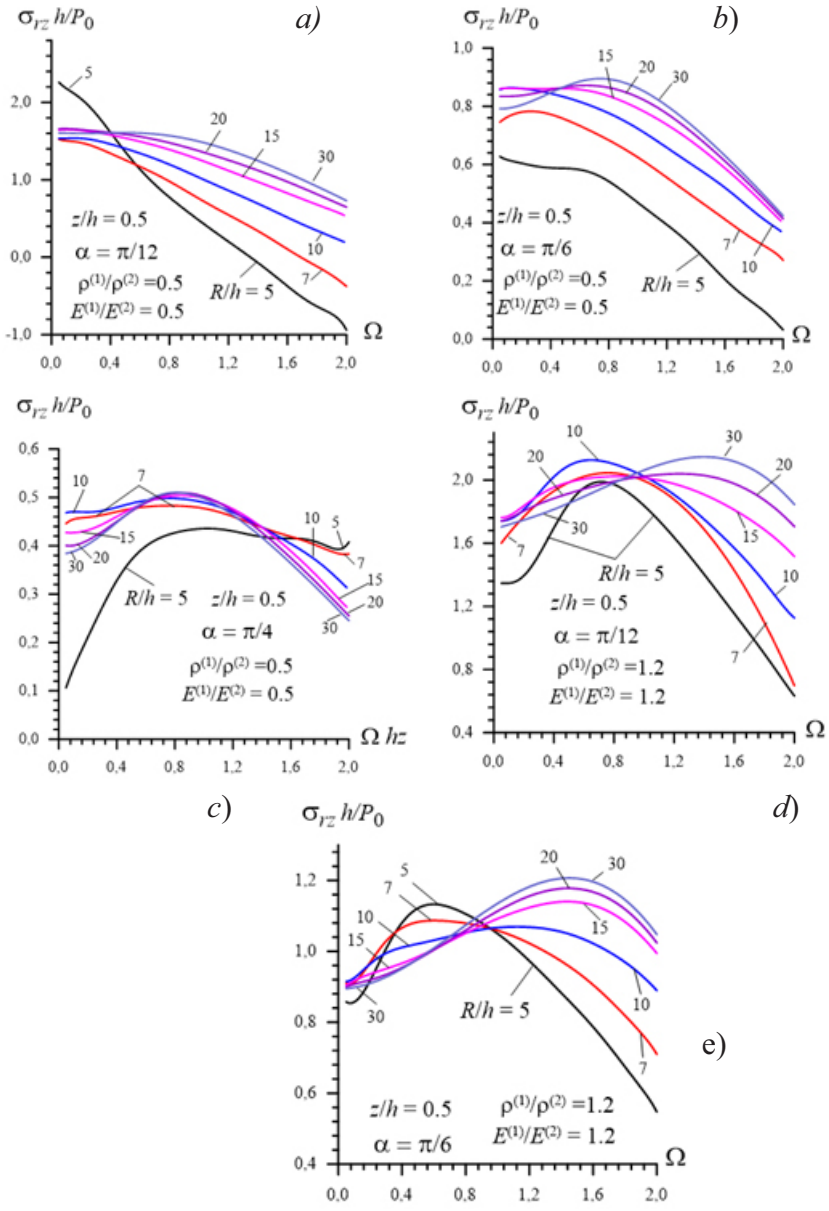

Fig. 3. The influence of the ratio R/h on t he frequency response of the interface shear stress σ_{rz} in the cases where $\alpha = \pi/12$ (a), $\pi/6$(b) and $\pi/4$(c) under $E^{(2.1)}/{}^{(2.1)}E^{(2.2)}$ $E^{(2.1)} = \rho^{(2.1)}/\rho^{(2.2)}) = 0.5$ and in the cases where $\alpha = \pi/12$ (d), $\pi/6$(e) under $E^{(1)}/E^{(2.2)} = \rho^{(1)}/\rho^{(2.2)}) = 1.2$.

Thus, it follows from the foregoing discussions that the character of the influence of the ratios $E^{(1)}/E^{(2)}$and R/hon the frequency response of the shear stress σ_{rz} is similar (in the qualitative sense) with that obtained for the normal stress σ_{rr} discussed in [4] and has the same explanation which are made in [4] for the results related to the σ_{rr} which is the interface normal stress.

Now we consider the results related to the frequency response of the circumferential shear stress $\sigma_{r\theta}$. These results are presented in Fig. 4 and 5 which illustrate the influence of the ratios $E^{(2.1)}/E^{(2.2)}$ (Fig. 4) and R/h (Fig. 5) on the mentioned frequency response. Under investigation the

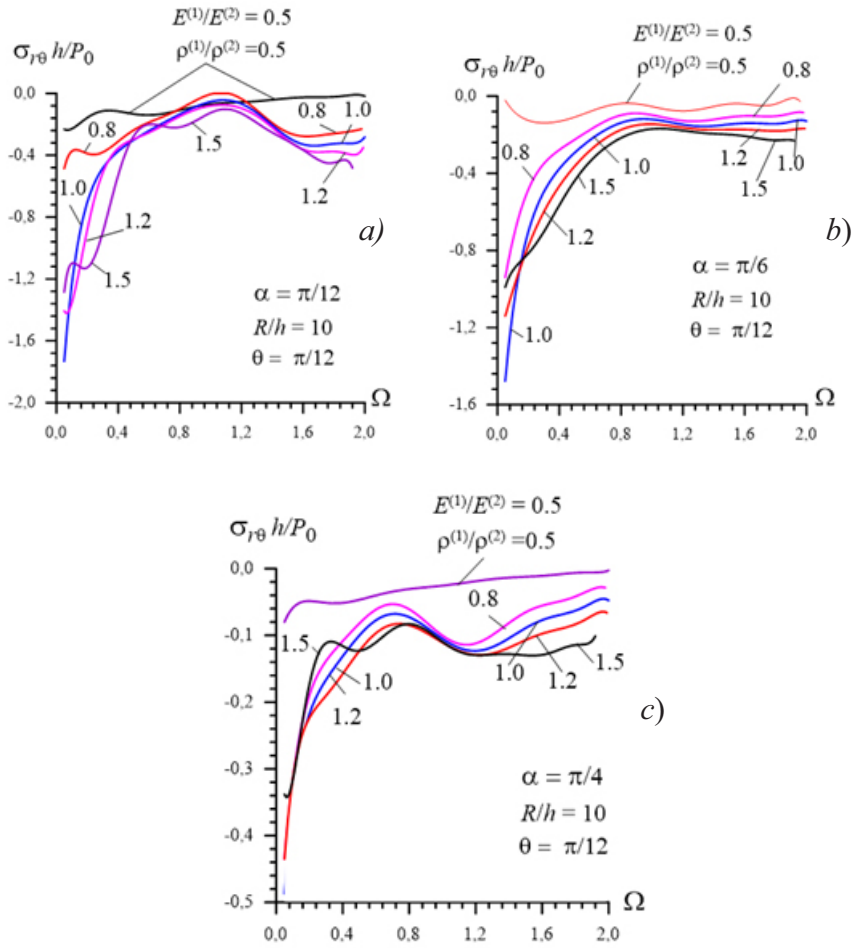

Fig. 4. Frequency response of the interface shear stress $\sigma_{r\theta}$ in the cases where $\alpha = \pi/12$ (a), $\pi/6$ (b) and $\pi/4$(c) for various values of the ratio $E^{(1)}/E^{(2)}(=\rho^{(1)}/\rho^{(2)})$ under $R/h = 10$

influence of the ration $E^{(1)}/E^{(2)}$on this response it is considered the cases where $\alpha = \pi/12$ (Fig. 4a), $\pi/6$(Fig. 4b) and $\pi/4$ (Fig. 4c) for $R/h = 10$, however under investigations the influence of the ratio R/hon this response it is considered the cases where $\alpha = \pi/6$ (Fig. 5a under $E^{(1)}/E^{(2)} = 0.5$ and Fig. 5c under $E^{(1)}/E^{(2)} = 1.2$) and $\alpha = \pi/4$ (Fig. 5b under $E^{(1)}/E^{(2)} = 0.5$ and Fig. 5d under $E^{(1)}/E^{(2)} = 1.2$). Note that the shear stress $\sigma_{r\theta}$ appears namely as a result of the non-axisymmetric external loading of the system under consideration and, according to the results given in Fig. 4 and 5, decrease with the angle α. Moreover, according to Fig. 5, it can be concluded that an increase in the values of the ratio $E^{(1)}/E^{(2)}$ causes an increase in the absolute values of the stress $\sigma_{r\theta}$ although there are some deviations from this decreasing. What is more these deviations appear for the relatively great values of the ratio $E^{(1)}/E^{(2)}$ (for instance, for the $E^{(1)}/E^{(2)} = 1.5$).

If follows from the results given in Fig. 5a and Fig. 5b (in Fig. 5c and Fig. 5d) the influence of the ratio R/h on the frequency response of the stress $\sigma_{r\theta}$ has complicate

character. Nevertheless, according to these results, we can conclude that in the case where $E^{(1)}/E^{(2)} = 0.5$ (in the case where $E^{(1)}/E^{(2)} = 1.2$) an increase of the ratio R/h causes an increase (a decrease) in the absolute maximum values of the stress $\sigma_{r\theta}$ with respect to the dimensionless frequency Ω. Moreover, these results also show that the values of the stress $\sigma_{r\theta}$ approach to each other with R/h.

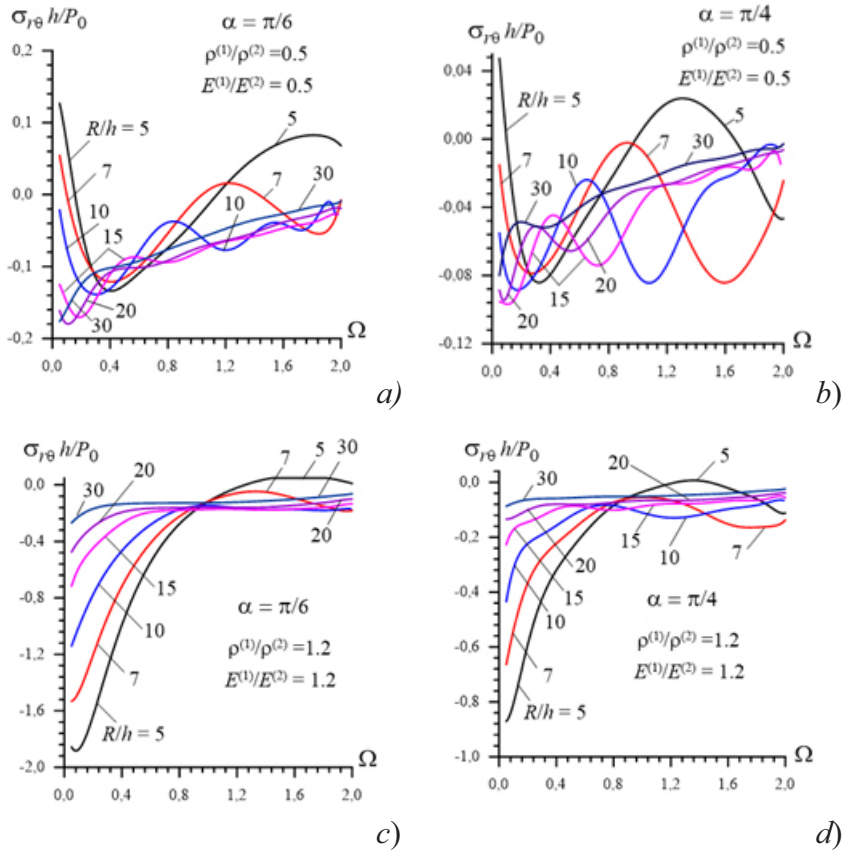

Fig. 5. The influence of the ratio R/h on the frequency response of the interface shear stress $\sigma_{r\theta}$ in the cases where $\alpha = \pi/6$ (a) and $\pi/4$(b) under $E^{(1)}/E^{(2)} = \rho^{(1)}/\rho^{(2)}) = 0.5$ and in the cases where $\alpha = \pi/6$ (d) and $\pi/4$(e) under $E^{(2)}/E^{(2)} = \rho^{(1)}/\rho^{(2)}) = 1.2$.

Consider distribution of the shear stress σ_{rz} with respect to the dimensionless coordinate z/h obtained for various angle α under $\theta = 0$. This distribution is illustrated by graphs given in Fig. 6 from which follows that this distribution is also has quasi-periodic character which similar with that observed for the normal stress σ_{rr} which is discussed in [4]. However, the "first" amplitude of this distribution is not absolute maximum of the stress σ_{rz} and this absolute maximum is the "second" amplitude of this distribution which appear at $z/h \approx 3.0$ (we recall that the first amplitude of the distribution of the normal stress σ_{rr} which appear at $z/h = 0$ [4] is the absolute maximum of the σ_{rr} with respect to z/h). Consequently, before a certain distance from the point at which the external force acts the amplitude of the distribution increases, however, after this point the amplitudes of theσ_{rz}decrease with z/h.

The distribution of the shear stress σ_{rz} at $z/h = 0.5$ with respect to the coordinate θ for various α are illustrated through the graphs given in Fig. 7 from which follows that this distribution is similar in the qualitative sense with that obtained for the normal stress σ_{rr} and shown in [4]. Nevertheless, in Fig. 7 the appearing of the maximums of the stress σ_{rz}in the cases where $\alpha = \pi/4$ and $\pi/2$ at $\theta = \theta'' > 0$ is observed more clearly than that in [4].

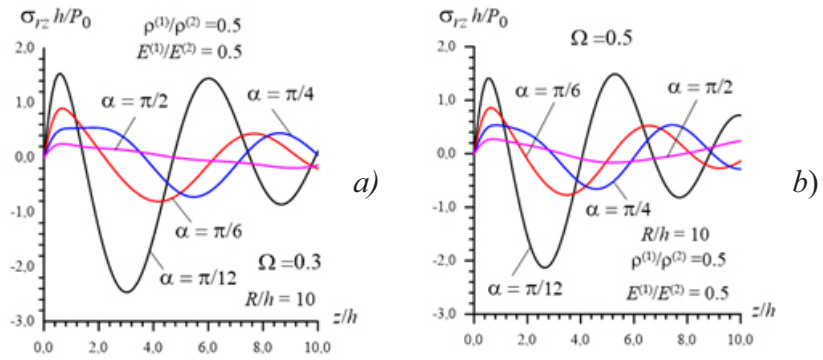

Fig. 6. The distribution of the interface shear stress σ_{rz} with respect to the coordinate z/h in the cases where $\Omega = 0.3$ (a) and 0.5 (b).

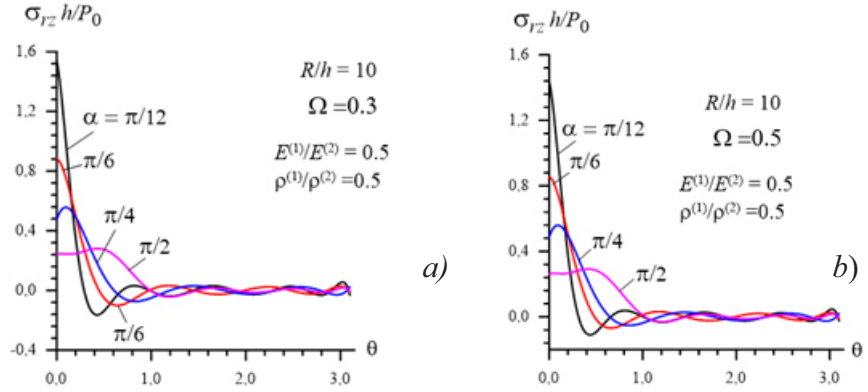

Fig. 7. The distribution of the interface shear stress σ_{rz} with respect to the coordinate θ in the cases where $\Omega = 0.3$ (a) and 0.5 (b).

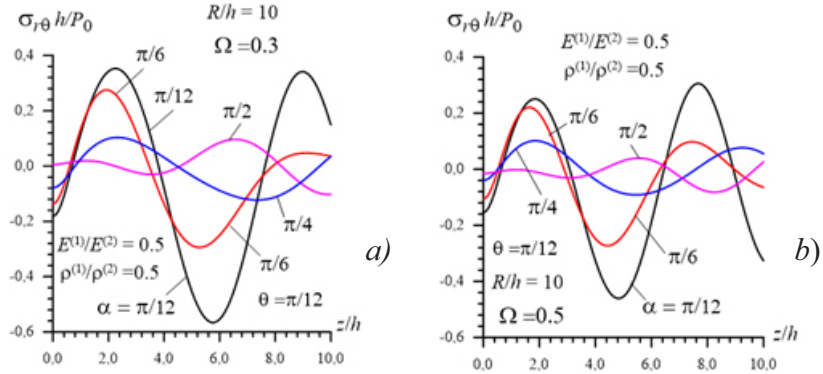

Fig. 8. The distribution of the interface shear stress $\sigma_{r\theta}$ with respect to the coordinate z/h in the cases where $\Omega = 0.3$ (a) and 0.5 (b)

Finally, we consider the distribution of the shear stress $\sigma_{r\theta}$ with respect to coordinates z/h and θ which are given in Fig.8 and 9 respectively. Note that under construction of the graphs given in Fig. 8 the values of the stress $\sigma_{r\theta}$ are calculated at $\theta = \pi/12$, however under construction of the graphs given in Fig. 9 the values of the this stress are calculated

at $z/h = 0$. It follows from Fig. 8 that the distribution of the stress $\sigma_{r\theta}$ with respect to the z/h is similar in the qualitative sense with that obtained for the shear stress σ_{rz}, i.e. the absolute maximum amplitude of the stress appear in a certain distance from the point at which the external forces acts and before (after) this point amplitudes of the distribution increase (decrease). However, Fig. 9 shows that the distribution of the shear stress $\sigma_{r\theta}$ with respect to the θ differ significantly from those obtained for the stressesσ_{rr} [4] and σ_{rz} (Fig. 7). It follows from the graphs given in Fig.9 that the absolute maximum of the stress $\sigma_{r\theta}$ appears at $\theta = \theta* > 0$ and the values of the $\theta*$ increase with angle α. Moreover these graphs show that the mentioned distribution has "vibrational" character and the amplitudes of this "vibration" decrease rapidly with θ.

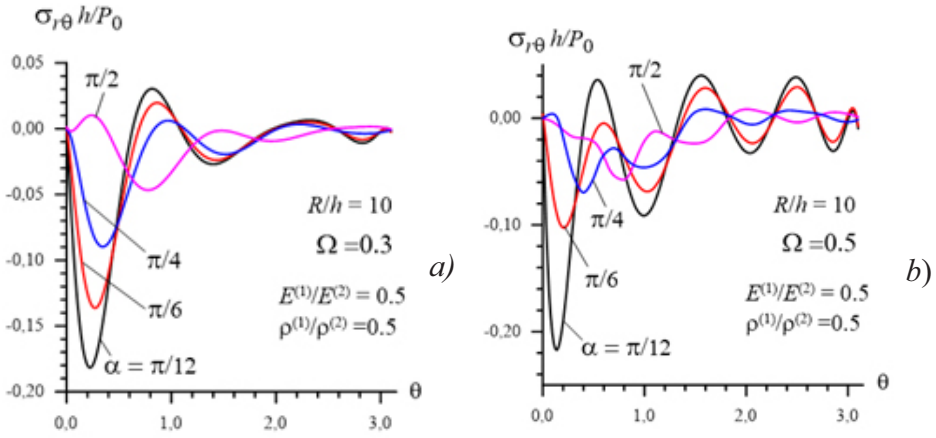

Fig. 9. The distribution of the interface shear stress $\sigma_{r\theta}$ with respect to the coordinate θ in the cases where $\Omega = 0.3$ (a) and 0.5 (b).

This completes the consideration and analysis of the numerical results.

4 Conclusions

According to these discussions, the following main and concrete conclusions can be drawn:

1 Absolute maximum values of amplitudes of the interface stresses obtained in the non-axisymmetric case are greater significantly than those obtained in the corresponding axisymmetric case;
2 An increase in a modulus of elasticity of the surrounding elastic medium (of the material of the hollow cylinder) under fixed modulus of elasticity of a modulus of elasticity of the hollow cylinder's material (of the surrounding elastic medium) cases an increase (a decrease) in the absolute values of amplitudes of the interface shear stresses;
3 Absolute values of amplitudes of the interface shear stresses increase monotonically with decreasing of the thickness (with increasing of the external radius of the cross section) of the hollow cylinder;
4 An increase of the central angle within which the external forces are distributed, causes a decrease in the absolute maximum values of the interface shear stresses;
5 Distributions of amplitudes of the interface shear stresses with respect to the axial coordinate has quasi-periodic character and period of these distributions increase, however the amplitudes decrease with the aforementioned central angle;
6 The character of the distribution of amplitudes of the interface shear stresses with respect to the circumferential coordinate depends significantly on the values of the aforementioned central angle.

References

1. Akbarov S.D., Mehdiyev M.A.: *Forced vibration of the elastic system consisting of the hollow cylinder and surrounding elastic medium under perfect and imperfect contact*. Struct Eng Mech, **62** (1), 113–123, (2017).
2. Akbarov S.D., Mehdiyev M.A.: *Influence of initial stresses on the critical velocity of the moving load acting in the interior of the hollow cylinder surrounded by an infinite elastic medium*, Struct Eng Mech, **66** (1), 45–59, (2018).
3. Akbarov S.D., Mehdiyev M.A., Ozisik M.: *Three-dimensional dynamics of the moving load acting on the interior of the hollow cylinder surrounded by the elastic medium.* Structural Engineering and Mechanics, **67** (2), 185–206, (2018).
4. Akbarov S.D., Mehdiyev M.A.: *The interface stress field in the elastic system consisting of the hollow cylinder and surrounding elastic medium under 3D non-axisymmetric forced vibration*, CMC: Computers, Materials & Continua, **54** (1), 61–81 (2018).
5. Akbarov S.D.: Dynamics of pre-strained bi-material elastic systems: Linearized three-dimensional approach. *Springer, Berlin* (2015).
6. Eringen A.C., Suhubi E.S.: Elastodynamics, Finite motion, **I**. Linear theory, **II**, *Academic Press, New-York* (1975).
7. Guz A.N.: Fundamentals of the three-dimensional theory of stability of deformable bodies, *Springer, Berlin* (1999).
8. Ozisik M., Mehdiyev M.A., Akbarov S.D.: *The influence of the imperfectness of contact conditions on the critical velocity of the moving load acting in the interior of the cylinder surrounded with elastic medium*, CMC: Computers, Materials & Continua, **54** (2), 103–136 (2018).